Constraints on the composition of the Martian south polar cap from gravity and topography

Mark A. Wieczorek

Institut de Physique du Globe de Paris, Equipe d'Etudes Spatiales et Planétaire

4 avenue de Neptune, Saint-Maur 94107 FRANCE (wieczor@ipgp.jussieu.fr, www.ipgp.jussieu.fr/~wieczor)

SUMMARY

- A localized cross-spectral analysis of gravity and topography over the Martian south polar layered deposits yields a best-fit density of 1251 kg m^{-3} for these volatile rich deposits, with 1-σ limits of 1157 and 1369 kg m^{-3}, respectively. The best fit elastic thickness associated with this young geologic load is 161 km, but any value greater than 110 km can fit the data.
- Up to 55% solid CO_2 by volume could be sequestered in the polar layered deposits if they were dust free. Alternatively, between 14 to 28% dust by volume could be sequestered in these deposits if they were completely free of CO_2.
- Reasonable estimates for the present-day Martian heat flow predict that solid CO_2 would have melted beneath the thicker portions of the polar cap. Depending on the quantity of CO_2 that is present in the polar caps, it is even possible that water ice could melt under current conditions.

1. THE SOUTH POLAR LAYERED DEPOSITS

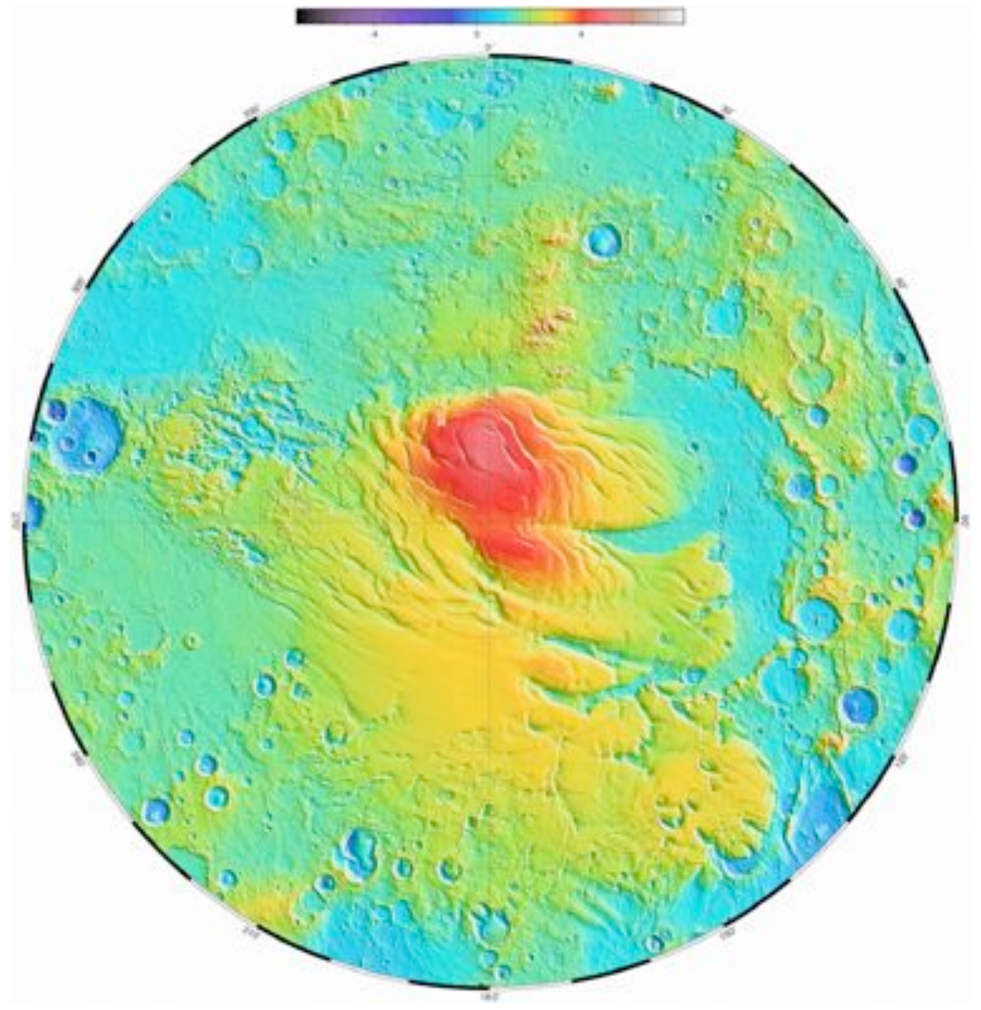

What do we know?

- The south polar cap retains a residual cover of CO_2 ice during the southern summer that is about 8 meters thick (e.g., *Byrne and Ingersoll*, 2003).
- Water ice appears to be abundant beneath the residual CO_2 cover (*Titus et al.*, 2003; *Bibring et al.*, 2004).
- Dust is present in various abundances on its surface, and is likely to be at least one cause for the visible layering of these deposits (e.g., *Langevin et al.*, 2005; *Douté et al.*, 2007).
- MARSIS-derived radar loss tangents can be interpreted as a mixture of water ice and 5% dust by volume (*Plaut et al.*, 2007).
- The morphology of the south polar cap is inconsistent with it being composed of 100% solid CO_2, which is rheologically weak (*Nye et al.*, 2000).

What don't we know?

- What is the absolute abundance of solid CO_2 in the south polar cap?
- What is the absolute abundance of dust in the south polar cap?
- How would solid CO_2 affect the radar loss tangent?
- What is the interior temperature of the south polar cap?

2. LOCALIZED CROSS-SPECTRAL ANALYSIS

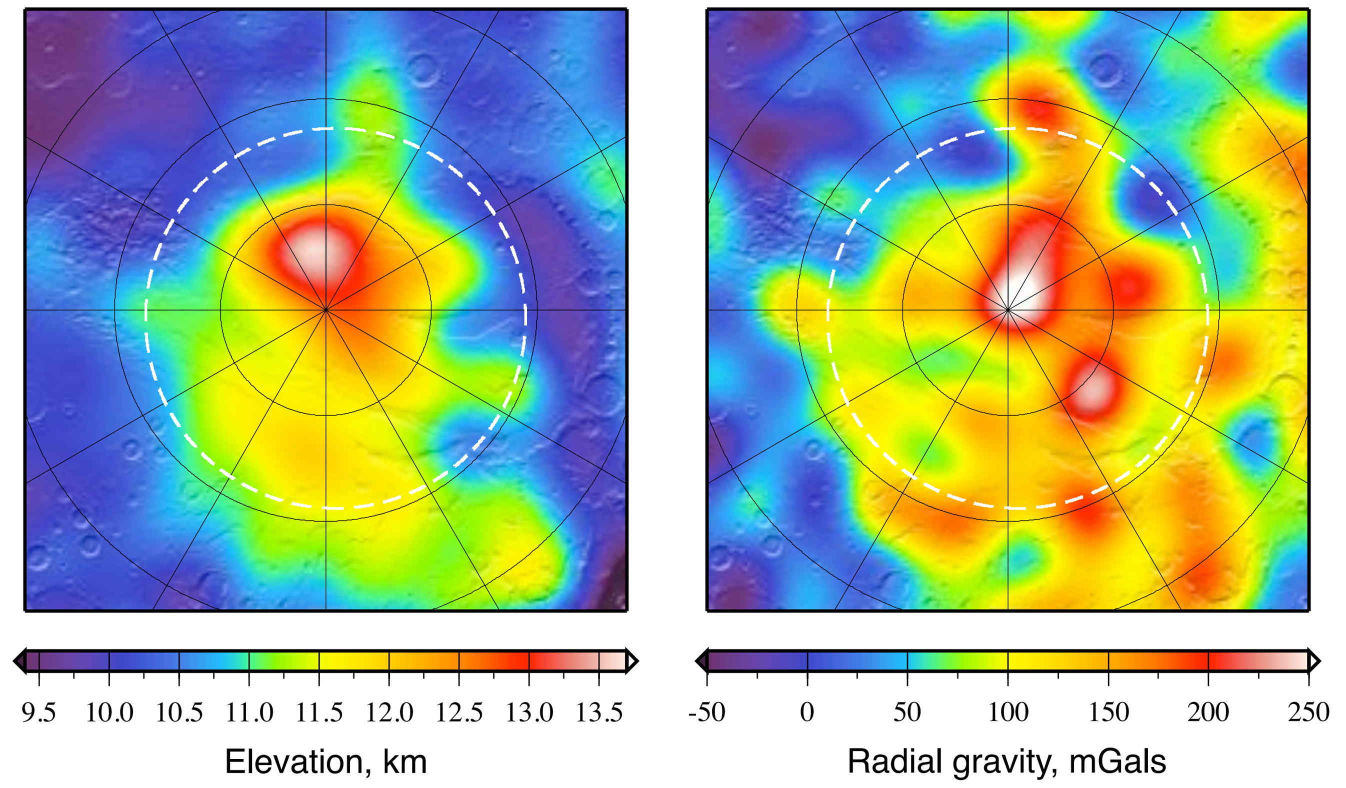

Figure 2. Topography (MarsTopo719) and radial gravity (MROMGM0020G) of the south polar region. Both images have been constructed using a maximum spherical harmonic degree of 75 and are referenced to the surface of a flattened ellipsoid that approximates the shape of Mars. The dotted circle with an angular radius of 9° corresponds to the region where the localized analysis was performed. Latitudinal grid lines in this polar stereographic projection are spaced every 5°, whereas longitudinal gridlines are spaced every 30°.

Why not perform a spatial analysis?

- Gravity and topography are only partially correlated in the space domain as a result of uncertainties in the gravity model and subsurface geologic processes.
- Before performing a spatial analysis, it is necessary to remove the global Tharsis load and flexure signal that is important up to at least degree 5 (see *Wieczorek and Zuber*, 2004).

Why perform a spectral analysis?

- While gravitational noise will bias the correlation spectrum downwards, it will not affect the admittance spectrum (unless the signal-to-noise ratio is close to unity).
- Subsurface geological processes that are uncorrelated with the surface topography will not bias the admittance function.
- Analysis of the degree-dependent spectral admittance function allows one to place constraints on both the ice cap density and lithospheric thickness.

How was it done?

- A single localization window that optimally concentrates 99% of its power within the region of interest was constructed using the methodology of *Wieczorek and Simons* (2005).
- Both the gravity g and topography f were multiplied by this window, the resulting functions Γ and Φ were expanded into spherical harmonics, the cross-power spectra were obtained

$$Z(l) = \frac{S_{\Phi\Gamma}(l)}{S_{\Phi\Phi}(l)} \qquad \gamma(l) = \frac{S_{\Phi\Gamma}(l)}{\sqrt{S_{\Phi\Phi}(l)S_{\Gamma\Gamma}(l)}}$$

3. RESULTS

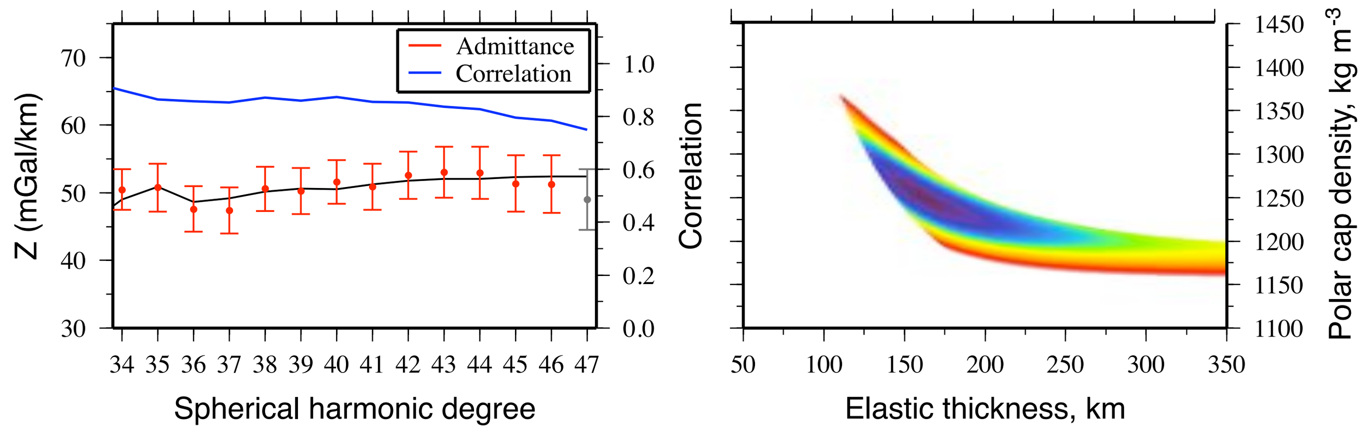

Figure 3. (Left) Localized admittance and correlation spectra obtained using a localization window with?θ = 9° and L = 28. Only degrees greater than L+5 and less than or equal to 75 - L are shown, where L is the spherical harmonic bandwidth of the localization window. The admittance is plotted in light gray where the correlation function is less than 0.775, which corresponds to a signal-to-noise ratio of 1.5. The best fitting model with ρ = 1251 kg m^{-3} and T_e = 161 km is shown in dark gray. (Right) Elastic thickness and polar cap density parameter space that fits the admittance at all degrees to one standard deviation. Dark colors indicate a better fit.

Analysis details

- The localized admittance for degrees less than or equal to L + 5 were ignored since these are influenced by the Tharsis load and flexural response.
- The localized admittance was ignored where the localized correlation function implied a signal-to-noise ratio less than 1.5. (The localized admittance was found to steadily decrease for lower signal-to-noise ratios.)
- The position of the localization window was chosen in order to maximize the localized correlation function.
- A localization window with an angular radius of 9° was chosen because (1) smaller windows yielded too few degrees to analyze, resulting in large uncertainties, and (2) larger windows contained some signal from the surrounding cratered terrain that is partially compensated, and hence not described by the theoretical model.
- Theoretical 3-D forward models were generated for a range of elastic thicknesses and polar cap densities. Those models that fit the observations at all degrees to one standard deviation are shown in the above figure.

The best-fit density for the polar layered deposits is 1251 kg m^{-3}, with 1-σ limits of 1157 and 1369 kg m^{-3}.

The best fit elastic thickness is 161 km, though any value greater than 110 km can fit the data.

These results are insensitive to reasonable variations in the reference crustal thickness, crustal density, and angular radius of the localization window. Furthermore, nearly identical results are obtained using both pre- and post-MRO gravity models.

- *Zuber et al.* (2007) estimated the density of the south polar layered deposits using a Cartesian method developed in the space domain combined with constraints on lithospheric flexure and ice thickness provided by MARSIS data, and assumptions about crustal compensation. They obtained a best-fit density of 1220 kg m^{-3} for these deposits with a 95% confidence interval of 740–1780 kg m^{-3}. For comparison, the 2-σ density limits of this spectral analysis are 1069 and 1626 kg m^{-3}.

4. COMPOSITION OF THE SOUTH POLAR CAP

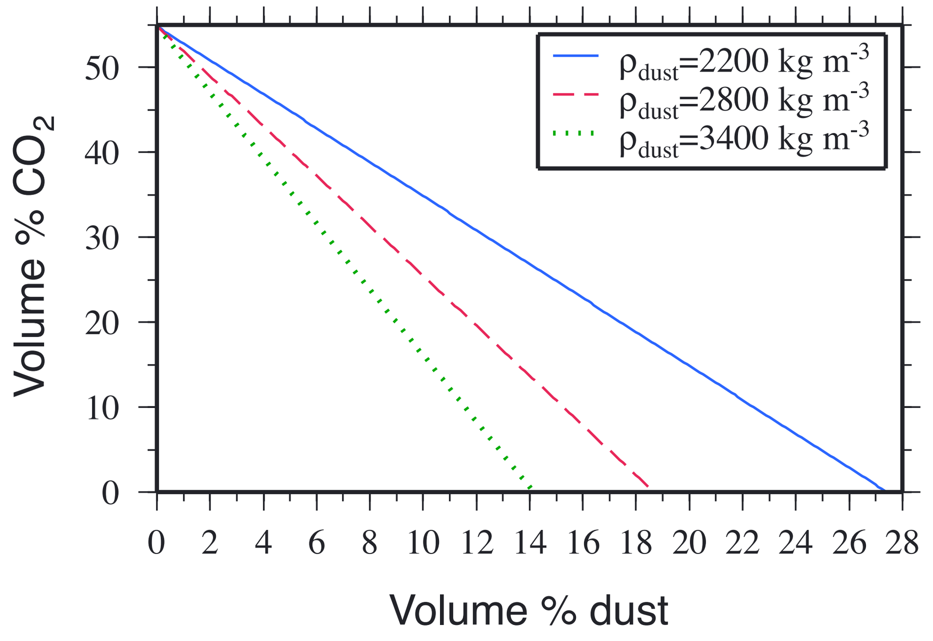

Figure 4. Allowable concentrations of solid CO_2 in the south polar layered deposits as a function of dust content. The bulk density of the polar layered deposits is assumed to be 1251 kg m^{-3}, and results are plotted using three possible densities of Martian dust.

- The densities of water ice and solid CO_2 are 920 and 1560 kg m^{-3}, respectively. If the polar cap were dust free, its best-fit density implies that it would be composed of 55% solid CO_2 by volume and 45% water ice.
- A reasonable range of densities for Martian dust is 2200 to 3400 kg m^{-3}. If the south polar cap were free of CO_2, it would contain between 14 and 28% dust by volume.

5. BASAL MELTING OF CO_2 AND WATER ICE

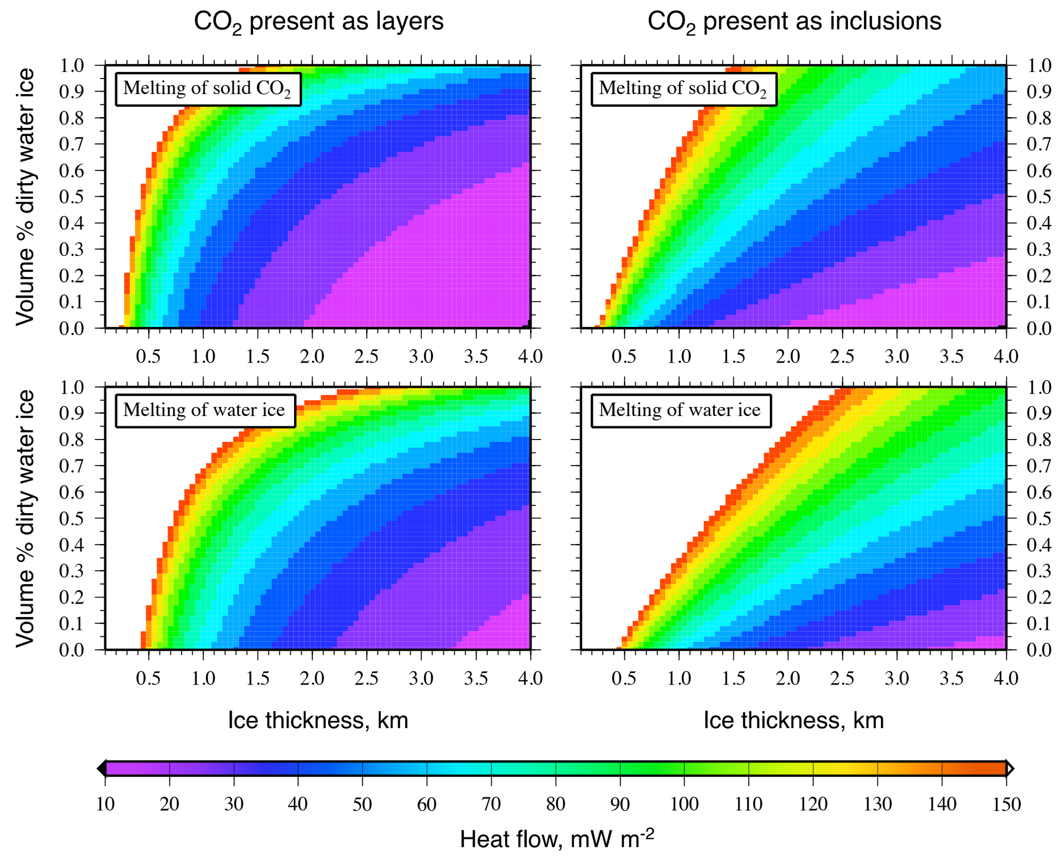

Figure 5. Critical heat flow required to initiate melting at the base of the south polar layered deposits as a function of ice cap thickness and volume % (dirty) water ice. Upper row is for the melting of solid CO_2 and the lower row is for the melting of water ice. Left column corresponds to the situation where dirty-water and dirty-dry ice are present as interbedded horizontal layers, and the right column is for the case where dirty dry ice is present as spherical inclusions in a dirty water-ice matrix. The surface temperature is assumed to be 155 K, 10% dust is incorporated in both the water and dry ice, and the melting temperatures of water and dry ice are assumed to be 273 and 216 K, respectively.

- The interior temperatures of the south polar cap depend upon its thermal conductivity and the planetary heat flow. The thermal conductivity of solid CO_2 is about 5 times less than water ice and this acts to increase the thermal gradient, possibly leading to the melting of either solid CO_2 or water ice. The largest temperatures arise when CO_2 is present as horizontal layers. The present day heat flow is probably between 25 and 35 mW m^{-2}.
- The presence of 10 to 30% solid CO_2 in horizontal layers would have caused this component to melt where the polar cap is thickest. Since liquid CO_2 is more dense than water ice, it would ultimately be sequestered in the underlying crust.
- The presence of more than 30% solid CO_2 in horizontal layers could cause water ice to melt where the cap is thickest. Esker-like structures suggest that basal melting probably occurred at some point in the past, perhaps when the ice cap was thicker.